Danilenko, Aleksandr; Rastgou, Masoud; Manoocheri, Farshid; Kinnunen, Jussi; Korpelainen, Virpi; Lassila, Antti; Ikonen, Erkki

Characterization of PillarHall test chip structures using a reflectometry technique

Published in:
Measurement Science and Technology

DOI:
10.1088/1361-6501/acda54

Published: 01/09/2023

Document Version
Publisher's PDF, also known as Version of record

Characterization of PillarHall test chip structures using a reflectometry technique

OPEN ACCESS
IOP Publishing

Measurement Science and Technology

Meas. Sci. Technol. **34** (2023) 094006 (7pp)

https://doi.org/10.1088/1361-6501/acda54

Characterization of PillarHall test chip structures using a reflectometry technique

Aleksandr Danilenko[1,*], **Masoud Rastgou**[1], **Farshid Manoocheri**[1], **Jussi Kinnunen**[2], **Virpi Korpelainen**[3], **Antti Lassila**[3] **and Erkki Ikonen**[1,3]

[1] Aalto University, Metrology Research Institute, Maarintie 8, 02150 Espoo, Finland
[2] Chipmetrics Oy, Yliopistokatu 7, 80130 Joensuu, Finland
[3] VTT MIKES, Tekniikantie 1, 02150 Espoo, Finland

E-mail: aleksandr.danilenko@aalto.fi

Received 15 January 2023, revised 17 May 2023
Accepted for publication 31 May 2023
Published 19 June 2023

Abstract

Thin film samples where one of the thin layers consists of a vacuum or air are called PillarHalls due to their support structure in silicon wafers. Custom PillarHall samples were provided by Chipmetrics Ltd and characterized by reflectometry with a Cary 7000 spectrometer. Data at 8° of angle of incidence were collected with p-polarization of the incident light within the wavelength range of 550–1800 nm. These data were then analyzed with a dedicated MATLAB code, using fitting software accompanying the transfer matrix method for calculation of the reflectance spectrum. Layer thicknesses and unknown refractive indices were chosen as fitted parameters. The oscillating reflectance spectrum of the PillarHall test chip yielded an air gap thickness of 86 nm with an estimated standard uncertainty of 5 nm. This is close to the nominal value of 100 nm. The results demonstrate that reflectometry data are sensitive to the thickness of the thin air layer deep inside the silicon structure.

Keywords: reflectometry, PillarHall, modeling, conformal thin film

(Some figures may appear in colour only in the online journal)

1. Introduction

Microminiaturization in nanoelectronics is gradually reaching its limit. Every new step of scaling integrated circuits becomes more challenging and expensive, while providing fewer improvements in terms of performance and power efficiency. This problem requires new solutions to be found. In past years, numerous researchers and companies have focused their attention and efforts on the study of new technologies related to 3D vertically stacked microstructures [1–6].

The development of new technologies in electronics is usually accompanied by studies of new materials. Since 3D vertically stacked microstructures are more complicated in shape than the structures used before, studies of new conformal thin film materials have become a high-priority task. Usually, these kind of studies are performed using traditional cross-sectioning of vertical trenches, which can create problems when at an industrial manufacturing scale, since this technique requires a lot of time for analysis and is thus expensive. The PillarHall test chip structure [7–9] is a solution that alleviates this problem, since it is technically less demanding and significantly reduces costs.

* Author to whom any correspondence should be addressed.

PillarHall samples enable a fast and accurate way to study coating processes and characterize ultra-high aspect ratio nanometrology products since peeling of the PillarHall ceiling reveals the coating for direct measurements. PillarHall test chips are created to test conformal thin-film materials, which are used to create vertical microstructures using atomic layer deposition (ALD) and chemical vapor deposition (CVD) processes. Before using PillarHall test chips, it is necessary to characterize the structure, for example, to determine the PillarHall height, providing a critical parameter for layer deposition studies.

This work is focused on analyzing PillarHall layer heights based on spectral reflectance measurements, which have earlier demonstrated their capability for accurate thin film thickness characterizations [10–14]. We aim to create and validate physical models of PillarHall sample reflectance for the development of a traceable measurement technique for the determination of structural dimensions and optical constants of thin layered samples.

2. Theoretical background

This section gives a theoretical background of the determination of layer thicknesses in thin-layer samples. For a light beam propagating from medium 1 to medium 2, reflectance and transmittance of the light may be described by Fresnel equations. For instance, the amplitude coefficients for a single reflection and transmission of p-polarized light from interface 12 are [15–17]

$$r_{12} = \frac{n_2 \cos\theta_1 - n_1 \cos\theta_2}{n_2 \cos\theta_1 + n_1 \cos\theta_2} \tag{1}$$

$$t_{12} = \frac{2 n_1 \cos\theta_1}{n_2 \cos\theta_1 + n_1 \cos\theta_2} \tag{2}$$

where n_1 and n_2 are the refractive indices of mediums; θ_1 and θ_2 are incidence and refraction angles.

A thin film usually has multiple reflections occurring, as presented in figure 1. In this case, the amplitude reflection coefficient is [18]

$$r = r_{12} + \frac{t_{12} t_{21} r_{23} \mathrm{e}^{\mathrm{i}\beta}}{1 - r_{21} r_{23} \mathrm{e}^{\mathrm{i}\beta}} \tag{3}$$

where $\beta = \frac{4\pi}{\lambda} n_2 d \cos\theta_2$ is the phase difference between rays reflected from interfaces 12 and 23. Parameters d and λ are the thickness of the thin film and the vacuum wavelength of light, respectively. The reflectance [19]

$$R = |r|^2 = \frac{r_{12}^2 + r_{23}^2 + 2 r_{12} r_{23} \cos\beta}{1 + r_{12}^2 r_{23}^2 + 2 r_{12} r_{23} \cos\beta} \tag{4}$$

describes oscillations as a function of layer thickness or wavelength because of the $\cos\beta$ function.

In the case of a multilayer structure, the transfer matrix method (TMM) [17, 20–25] is a versatile tool for numerical calculations. The TMM supposes that every layer j of the structure is associated with a 2×2 matrix M_j with elements m_{11}, m_{12}, m_{21} and m_{22}. These matrix elements depend on incidence angle, complex refractive index, wavelength and thickness of the layer. After multiplication of all M_j matrices related to each layer, we get the total matrix M_{tot}. Using elements of this matrix, the reflectance can be calculated. Equation (4) is the result when applying TMM in the case of a single thin layer.

Thus, with the knowledge of the thickness and refractive index of each thin layer, we can use the TMM to calculate the reflectance spectrum within a certain wavelength range at a given angle of incidence. Our MATLAB software enables fitting of thicknesses and refractive indices to values that give minimal differences between simulated and measured reflectance curves.

3. Structure of the PillarHall chip

The PillarHall chip and its cross section are schematically shown in figure 2 [7]. A test structure is created to perform conformality measurements of thin film materials in ALD and CVD processes [8, 9]. Once the coating is completed, the upper membrane layer can be removed and the coating quality, i.e. uniformity and penetration depth, can be characterized.

PillarHall test structures of size of 15 mm $\times$ 20 mm are produced on silicon wafer substrates with thickness around 400 µm. The nominal vertical dimensions [7] of the PillarHall structure in this experiment are 1500 nm for the thickness of the polycrystalline silicon membrane (PolySi in figure 2) and 100 nm for the air gap between the PolySi membrane and the silicon substrate. The thin membrane is supported by pillars of 4 µm diameter at the distance of 49 µm from each other. When looked at from above, the area of pillars corresponds to approximately 0.5% of the total area of the test structure.

4. Measurement setup

Reflectometry measurements of PillarHall samples were performed using a Cary 7000 spectrometer [26]. The measurements were carried out with an incidence angle of 8° over the wavelength range of 550 nm–1800 nm (figure 3). The light beam of dimensions 3.5 mm $\times$ 8 mm was polarized in the plane of incidence (p-polarization). The bandwidth of the monochromator was 4 nm over the whole wavelength range.

5. Analysis of reflectometry data

5.1. Input data and fitting software

Measurement data were analyzed with a dedicated MATLAB code, which uses the TMM to calculate the reflectance from a layer-structured sample (see section 2). To create the layer

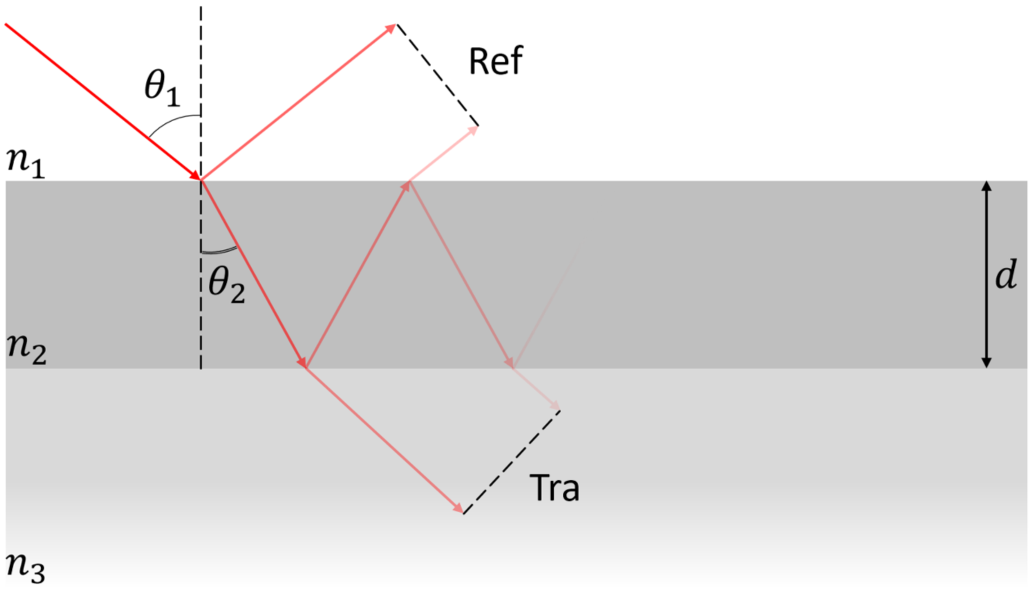

Figure 1. Multiple transmission and reflection in a thin film.

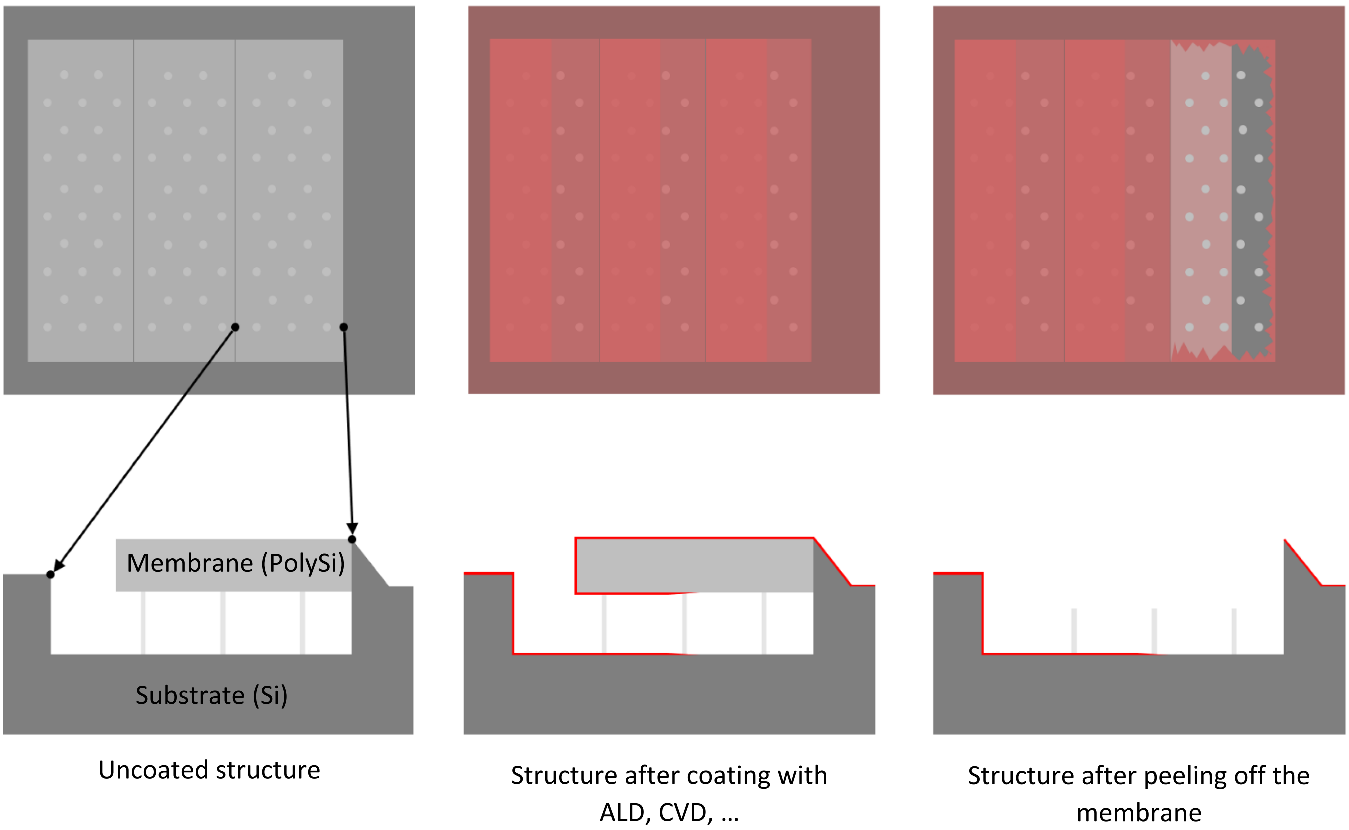

Figure 2. Top view of the PillarHall chip (top row) and side view of one of the PillarHall sections (lower row) for uncoated, coated and peeled-off structures. The corresponding points for the top and side views are shown with arrows. Penetration of the coating layer (shown as red) can be studied in high-aspect-ratio structures. The dimensions in figures 2, 4 and 7 are not drawn to the scale of real PillarHall samples.

model of the sample, the program requires material data such as tabular values of the real (n) and imaginary (k) parts of the refractive index at each wavelength and initial layer thickness values combined with upper and lower bounds. It is also possible that n and k are described with formulas including parameters for fitting.

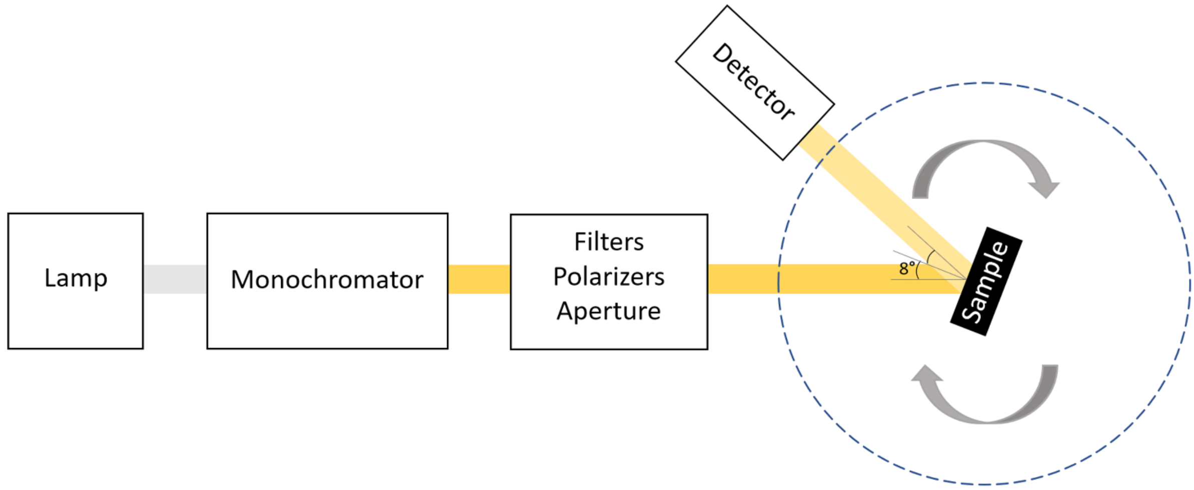

Figure 3. Schematic representation of the measurement setup.

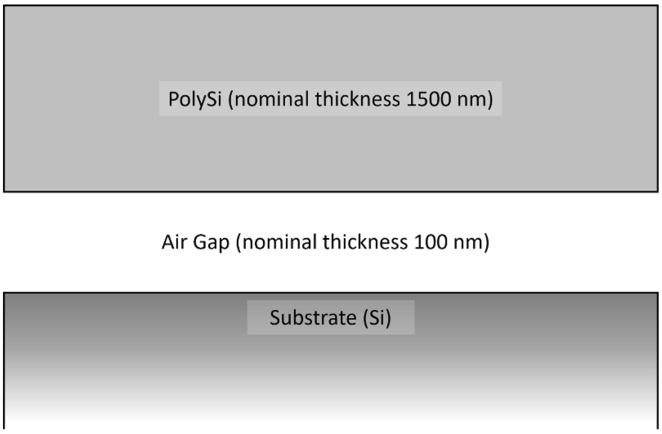

Figure 4. Two-layer PillarHall model with nominal thickness values.

5.2. Two-layer model

Analysis of the results of reflectometry measurements was started with the two-layer model shown in figure 4, in analogy with the structure of figure 2. The fitting software calculates reflectance according to the created layer model and measured beam parameters as shown in figure 5. The fitted parameters include the thicknesses of the air gap and the PolySi layer and the complex refractive index (n–ik) of the PolySi layer. Refractive indices of silicon substrate [27] and air are kept fixed. In order to describe the fitted refractive index curves, simplified Sellmeier equations [10] for n and k were employed. Fitted curves of n and k of PolySi versus silicon are presented in figure 6. The real part n is smaller for the PolySi layer than for bulk silicon, whereas k is larger for PolySi than for silicon. These results suggest that the PolySi layer has lower density than bulk silicon and higher absorbance of light than silicon in this wavelength range.

The fitted air gap thickness is 86 nm and the PolySi layer thickness is 1641 nm. The thickness parameters are mainly determined by the frequency and phase of the oscillation in figure 5, where a good agreement is obtained between the data and the fit. The mean difference between the measured and fitted reflectance is 2.3%. There are deviations at the peaks of the oscillation, and in the wavelength range of 550–700 nm there is a systematic deviation between the curves. Due to the short penetration depth of light in PolySi in this wavelength range, the systematic deviation indicates that the uppermost part of the layer model of figure 4 needs to be improved.

5.3. Three-layer model

Polycrystalline silicon, due to its structure and manufacturing process, consists of crystals of different sizes, placed in random orientations. As a result, the PolySi layer includes minor cavities that can contain gas, especially close to the surface. In order to improve the fitting of figure 5 at short wavelengths, one more layer of porous PolySi (pPolySi) was added to the layer model, as shown in figure 7.

Determination of the effective refractive index n_{eff} of the porous layer is based on the Bruggeman effective medium approximation [28–31]. It is calculated using the refractive index of host material n_{h} (PolySi), refractive index of voids (air) n_{v} and volume fraction f_{v} of voids, according to equation:

$$n_{\mathrm{eff}} = \sqrt{\frac{b + \sqrt{b^2 + 8c}}{4}}, \tag{5}$$

where

$$b = 3(1 - f_{\mathrm{v}})(n_{\mathrm{h}}^2 - n_{\mathrm{v}}^2) + 2n_{\mathrm{v}}^2 - n_{\mathrm{h}}^2 \tag{6}$$

and

$$c = n_{\mathrm{h}}^2 n_{\mathrm{v}}^2. \tag{7}$$

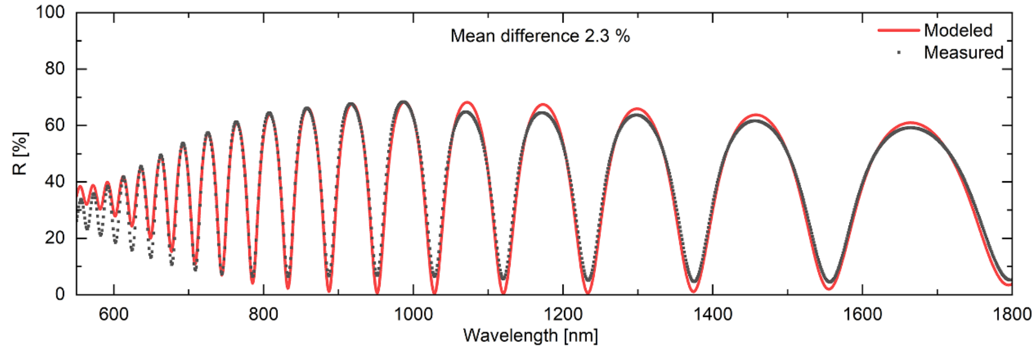

Figure 5. Measured reflectance data and fitting results for the two-layer PillarHall model in figure 4.

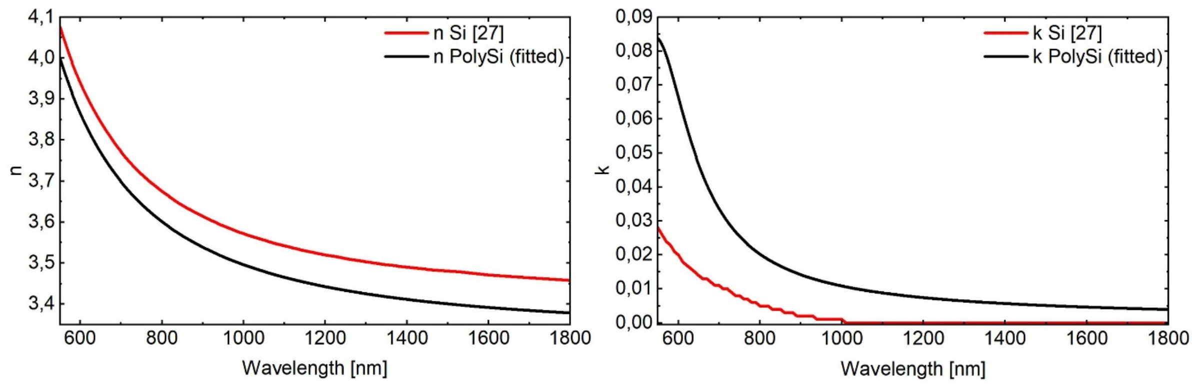

Figure 6. Fitted real (n) and imaginary (k) parts of the refractive index of PolySi for the two-layer model in figure 4, in comparison with the refractive index of silicon.

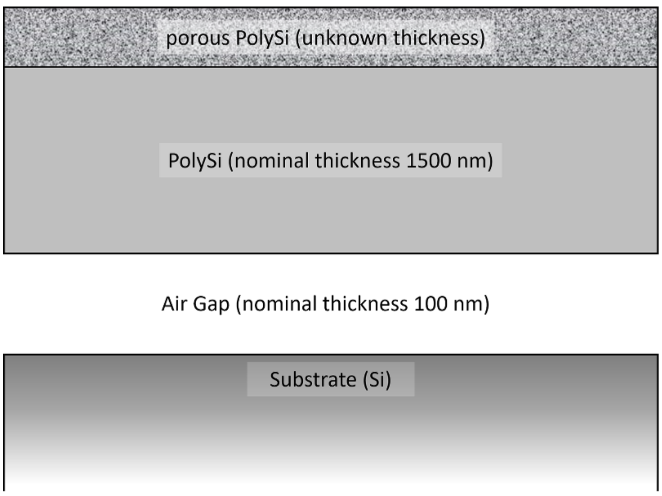

Figure 7. Three-layer PillarHall model with nominal thickness values.

After introducing the pPolySi layer on top of the PillarHall sample to correct for the deviation in the 550–700 nm range, it can be questioned if it is possible to describe the relatively thick PolySi layer with a single fitted thickness parameter. Simulation tests show that the phase shift of the oscillation minima in the range from 900 nm to 1800 nm in figure 5 is especially sensitive to the PolySi layer thickness. Since the measurement beam has dimensions of 3.5 mm $\times$ 8 mm, it is unlikely that the thickness of the PolySi layer is uniform within this spot size. Thus, the fitting of the three-layer model is improved by allowing a narrow uniform distribution of thickness values of the PolySi layer around the fitted average value.

For the fitted reflectance spectrum of the three-layer model shown in figure 8, the same air gap thickness of 86 nm as in the case of the two-layer model was found. The PolySi layer has a rectangular distribution of thickness values between 1590 nm and 1610 nm within the beam size. The thickness of the polySi layer is 21 nm with a volume fraction of 31%. The total thickness of the PolySi and pPolySi layers is 1620 nm, which is close to the nominal value of 1500 nm and the value of 1641 nm from the two-layer model. The mean difference between the data and the model reduces to 1.7 %. Fitted curves of n and k of pPolySi and PolySi versus silicon are presented in figure 9.

A sensitivity analysis of the air gap thickness was performed by fixing the air gap thickness to a varied value deviating from the fitted result of 86 nm and fitting the rest of the thicknesses to their optimal values. When the deviation of the fixed air gap thickness is manually increased or decreased from the optimal value of 86 nm and the rest of the thicknesses are fitted, the quality of the fit (i.e. mean difference) gradually becomes worse as compared with the fit of figure 8. At a deviation of $\pm$5 nm, there is a clear visible difference to the fit of figure 8. Thus, the final value of the air gap thickness with its standard uncertainty was obtained as (86 $\pm$ 5) nm, quite close to the nominal value of 100 nm.

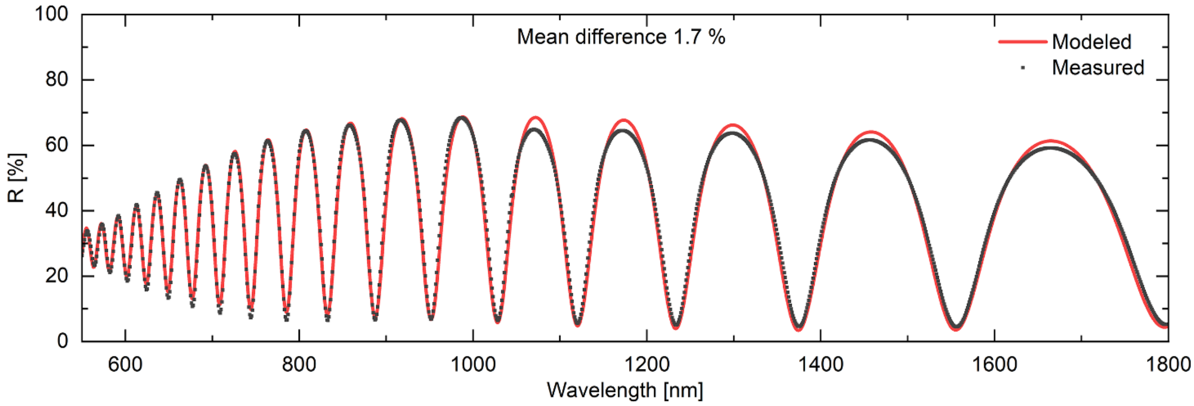

Figure 8. Measured reflectance data and fitting results for the three-layer PillarHall model in figure 7.

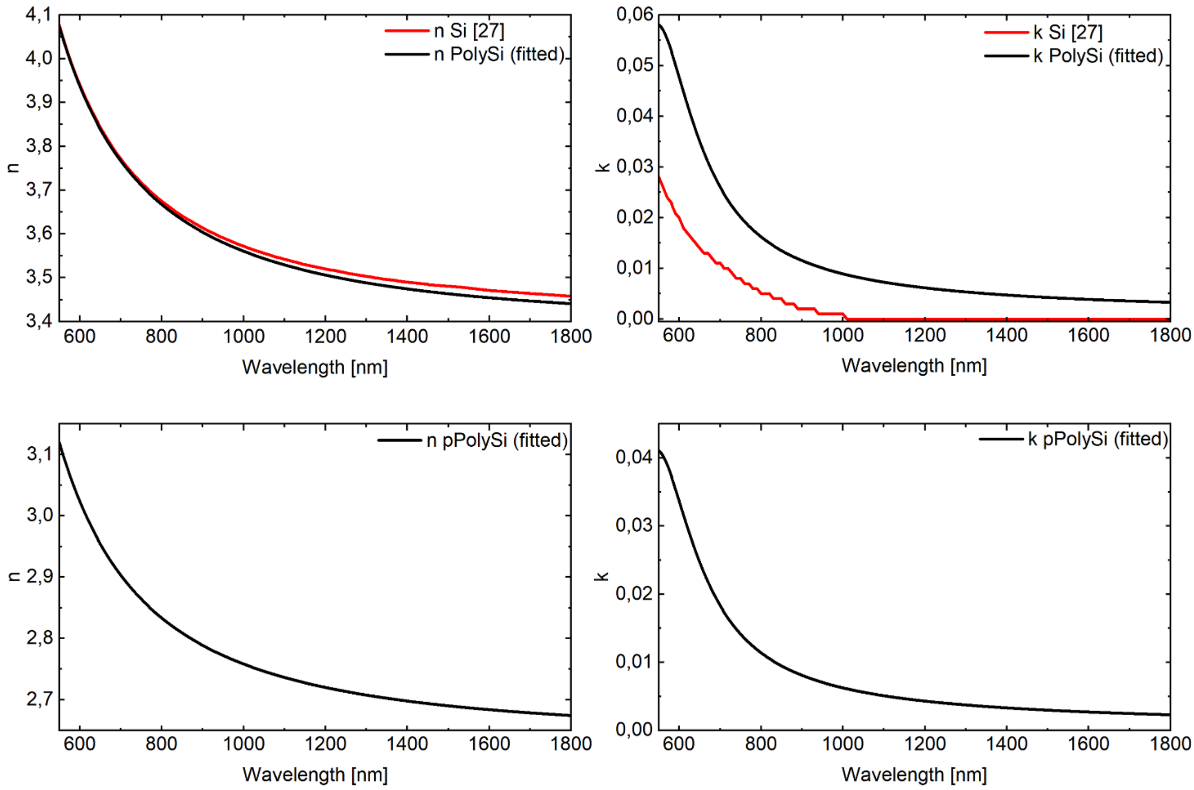

Figure 9. Fitted real (n) and imaginary (k) parts of the refractive index of PolySi for the three-layer model, in comparison with the refractive index of silicon (top row). Fitted real (n) and imaginary (k) parts of the effective refractive index of pPolySi (lower row).

6. Conclusions

In this paper, a PillarHall sample with nominal 100 nm air gap was characterized by reflectometry. Initially, a two-layer model, which corresponds to the nominal PillarHall structure, was used to fit the reflectometry data. The observed deviation between the fit and data at short wavelengths indicates that the layer model needs to be improved at the upper surface of the PillarHall sample. A three-layer PillarHall model, where the top layer is porous polycrystalline silicon and the total polycrystalline thickness is described by a narrow distribution around the central value, improves the quality of the fit and leads to the final value of the air gap thickness of (86 ± 5) nm. The air gap thickness is an important parameter for the users of PillarHall test chips.

It is shown here that measurement results obtained by reflectometry are sensitive to the thickness of the thin air layer deep inside the silicon structure. Infrared radiation at suitable wavelengths penetrates the silicon sample where reflection from the sample interfaces provides sufficiently detailed information on the layer structure. Such information is challenging to obtain with any other measurement method.

Data availability statement

All data that support the findings of this study are included within the article (and any supplementary files).

Acknowledgments

The project 20IND04 ATMOC leading to this publication has received funding from the European Metrology Programme for Innovation and Research (EMPIR) co-financed by the participating states and the European Union's Horizon 2020 research and innovation program. We also acknowledge support by the Academy of Finland Flagship Programme, Photonics Research and Innovation (PREIN), Decision Number: 320167.

ORCID iDs

Aleksandr Danilenko https://orcid.org/0000-0002-6662-7821
Antti Lassila https://orcid.org/0000-0002-6991-7082

References

[1] Then H W *et al* 2019 3D heterogeneous integration of high performance high-K metal gate GaN NMOS and Si PMOS transistors on 300mm high-resistivity Si substrate for energy-efficient and compact power delivery, RF (5G and beyond) and SoC applications *2019 IEEE Int. Electron Devices Meeting (IEDM)* (https://doi.org/10.1109/iedm19573.2019.8993583)
[2] Ishihara R *et al* 2012 Monolithic 3D-ICs with single grain Si thin film transistors *2012 IEEE 11th Int. Conf. on Solid-State and Integrated Circuit Technology* (*Xi'an, China*) (https://doi.org/10.1109/ICSICT.2012.6467714)
[3] Veloso A *et al* 2016 Challenges and opportunities of vertical FET devices using 3D circuit design layouts *2016 IEEE SOI-3D-Subthreshold Microelectronics Technology Unified Conf. (S3S)* (*Burlingame, CA, USA*) (https://doi.org/10.1109/S3S.2016.7804409)
[4] Al-Ameri T *et al* 2016 Performance of vertically stacked horizontal Si nanowires transistors: a 3D Monte Carlo/2D Poisson Schrodinger simulation study *2016 IEEE Nanotechnology Materials and Devices Conf. (NMDC)* (*Toulouse, France*) (https://doi.org/10.1109/NMDC.2016.7777117)
[5] Dey S, Jena J, Mohapatra E, Dash T P, Das S and Maiti C K 2019 Design and simulation of vertically-stacked nanowire transistors at 3nm technology nodes *Phys. Scr.* **95** 014001
[6] Kim S, Seo J, Choi J and Yoo H 2022 Vertically integrated electronics: new opportunities from emerging materials and devices *Nano-Micro Lett.* **14** 201
[7] Yim J, Ylivaara O M E, Ylilammi M, Korpelainen V, Haimi E, Verkama E, Utriainen M and Puurunen R L 2020 Saturation profile based conformality analysis for atomic layer deposition: aluminum oxide in lateral high-aspect-ratio channels *Phys. Chem. Chem. Phys.* **22** 23107–20
[8] Utriainen M *et al* 2022 Optical metrology of 3D thin film conformality by LHAR chip assisted method *Proc. SPIE* **12008** 120080D
[9] Arts K, Utriainen M, Puurunen R L, Kessels W M M and Knoops H C M 2019 Film conformality and extracted recombination probabilities of O atoms during plasma-assisted atomic layer deposition of SiO_2, TiO_2, Al_2O_3 and HfO_2 *J. Phys. Chem.* C **123** 27030–5
[10] Dobrowolski J A, Ho F C and Waldorf A 1983 Determination of optical constants of thin film coating materials based on inverse synthesis *Appl. Opt.* **22** 3191
[11] Lamminpää A, Nevas S, Manoocheri F and Ikonen E 2006 Characterization of thin films based on reflectance and transmittance measurements at oblique angles of incidence *Appl. Opt.* **45** 1392
[12] Friedrich K, Wilbrandt S, Stenzel O, Kaiser N and Heinz Hoffmann K 2010 Computational manufacturing of optical interference coatings: method, simulation results, and comparison with experiment *Appl. Opt.* **49** 3150
[13] Pourjamal S, Mäntynen H, Jaanson P, Rosu D M, Hertwig A, Manoocheri F and Ikonen E 2014 Characterization of thin-film thickness *Metrologia* **51** S302–8
[14] Holtslag A H M and Scholte P M L O 1989 Optical measurement of the refractive index, layer thickness, and volume changes of thin films *Appl. Opt.* **28** 5095
[15] Born M and Wolf E 2002 *Principles of Optics: Electromagnetic Theory of Propagation, Interference and Diffraction of Light* 7th edn (Cambridge: Cambridge University Press)
[16] Byrnes S J 2016 Multilayer optical calculations (arXiv:1603.02720)
[17] Furman S 1996 Basics of optics of multilayer systems. Atlantica Seguier Frontieres
[18] Haapalinna A, Manoochehri F and Ikonen E 1999 High-accuracy measurement of specular spectral reflectance and transmittance *Anal. Chim. Acta* **380** 317–25
[19] Ikonen E *et al* 2017 *Fundamentals of Optics* 6th edn (Tartu, Estonia: ScienceMosaic Publishing)
[20] Mohammed Z H 2019 The Fresnel coefficient of thin film multilayer using transfer matrix method TMM *IOP Conf. Ser.: Mater. Sci. Eng.* **518** 032026
[21] Fowles G R 1989 *Introduction to Modern Optics* 2nd edn (New York: Dover Publications)
[22] Hecht E 1998 *Optics* 3rd edn (New York: Addison-Wesley)
[23] Macleod H A 1986 *Thin-Film Optical Filters* (Tucson, AZ: A. Hilger Ltd)
[24] Wilford N H 1968 Electric fields produced by the propagation of plane coherent electromagnetic radiation in a stratified medium *J. Opt. Soc. Am.* **58** 380–90
[25] Luce A, Mahdavi A, Marquardt F and Wankerl H 2022 TMM-Fast, a transfer matrix computation package for multilayer thin-film optimization: tutorial *J. Opt. Soc. Am. A* **39** 1007–13
[26] Agilent Technologies, Inc. 2013 Agilent Cary Universal Measurement Accessory (UMA)
[27] Green M A 2008 Self-consistent optical parameters of intrinsic silicon at 300K including temperature coefficients *Sol. Energy Mater. Sol. Cells* **92** 1305–10
[28] Bruggeman G 1935 Calculation of various physics constants in heterogeneous substances I dielectricity constants and conductivity of mixed bodies from isotropic substances *Ann. Phys.* **416** 636–64
[29] Choy T C 1999 *Effective Medium Theory* (Oxford: Clarendon)
[30] Sela M and Haspel C 2020 Predicting the refractive index of amorphous materials using the Bruggeman effective medium approximation *Appl. Opt.* **59** 8822–7
[31] Khardani M, Bouaïcha M and Bessaïs B 2007 Bruggeman effective medium approach for modelling optical properties of porous silicon: comparison with experiment *Phys. Status Solidi* c **4** 1986–90